



14TH CANADIAN MASONRY SYMPOSIUM
MONTREAL, CANADA
MAY 16TH – MAY 20TH, 2021



SEISMIC BEHAVIOUR OF TALL REINFORCED MASONRY BUILDINGS

Hsu, Yu-Cheng¹; Yang, T.Y.² and Brzev, Svetlana³

ABSTRACT

Reinforced masonry (RM) has been used in Canada for more than 50 years, mostly for construction of low- and mid-rise buildings. The National Building Code of Canada 2015 (NBC 2015) permits the use of Ductile Shear Wall class for tall masonry buildings, but the height limit was set to 60 m at sites with moderate seismic hazard and 40 m for high seismic hazard sites. Only a few tall (15+ storey high) RM buildings have been constructed in Canada to date, mostly at sites with low to moderate seismic hazard. This paper provides an overview of past research studies on seismic response of Tall Reinforced Masonry (TRM) shear walls, and the governing parameters which are expected to influence their seismic response. The review also covers research on TRM buildings at the system level, and includes the studies on TRMs subjected to quasi-static loading and shaking table testing. Hybrid simulation approach has been proposed as an alternative to alternative seismic testing methods for TRM buildings. Hybrid simulation offers an opportunity for gaining an insight into the seismic response of entire TRM buildings by performing physical testing of portions of a single TRM wall, while the effect all other building components are simulated numerically. The authors are currently performing a comprehensive research program at the University of British Columbia to study the seismic response of TRM buildings subjected to earthquake excitation through hybrid simulation. This is believed to be the first application of hybrid technology in a research study on TRM wall structures in Canada and internationally.

KEYWORDS: *reinforced masonry, shear walls, tall buildings, seismic design, seismic behaviour, hybrid testing*

¹ PhD student, Department of Civil Engineering, The University of British Columbia, 6250 Applied Science Ln #2002, Vancouver, BC, Canada, ychsu11@mail.ubc.ca

² Professor, Department of Civil Engineering, The University of British Columbia, 6250 Applied Science Ln #2002, Vancouver, BC, Canada, yang@civil.ubc.ca

³ Adjunct Professor, Department of Civil Engineering, The University of British Columbia, 6250 Applied Science Ln #2002, Vancouver, BC, Canada, sbrzev@mail.ubc.ca

INTRODUCTION

Reinforced masonry (RM) has been used for construction of low- and mid-rise buildings in Canada for more than 50 years. A few tall RM buildings were constructed at sites with low to moderate seismic hazard in central and eastern Canada. For example, a 24-storey RM apartment building in Winnipeg, Manitoba, was built in the 1970s, and a few 21-storey RM apartment buildings were built in Hamilton, Ontario [1]. There are also a few tall RM applications in high seismic hazard areas of Canada. For example, three 16-storey RM buildings in Vancouver, British Columbia, were constructed in 1960s. Besides Canada, there are a few reported tall RM masonry building applications in the USA. For example, the 28-storey Excalibur Hotel in Las Vegas, Nevada (a low seismic hazard area) was constructed in 1989 [2]. A few tall RM buildings have also been reported in other countries, e.g., several 20-storey buildings in Brazil [3] and a 28-storey office building in Heilongjiang Province, China [4]. It is evident that the application of RM construction in high-rise buildings in moderate-to-high seismic hazard areas is limited, which can be attributed to limited compressive strength of commercially available concrete blocks and a lack of research studies related to seismic behaviour of TRM buildings [5].

Ductile detailing provisions for RM shear walls contained in the Canadian masonry design standard CSA S304 were last updated in 2014 (CSA S304-14) [6]. Provisions related to Moderately Ductile Shear Wall (MDSW) class with ductility force modification factor $R_d=2.0$ were revised, and a new class Ductile Shear Walls ($R_d=3.0$) was introduced. MDSW class is most common for seismic design applications in Canada, and is mandatory for all post-disaster buildings according to the National Building Code of Canada 2015 (NBC 2015) [7] and CSA S304-14 [6]. Partially grouted MDSWs can be used at sites with low seismic hazard level, where wall aspect ratio is not larger than 2.0, and also at sites with higher seismic hazard with the axial precompression stress less than $0.1f'_m$, where f'_m denotes the masonry compressive strength. Fully grouted MDSWs are required at sites with high seismic hazard. The CSA S304-14 seismic design provisions for RM shear walls are explained and illustrated through design examples by Brzev and Anderson [8]. NBC 2015 [7] permits the use of Moderately Ductile and Ductile Shear Wall classes for RM buildings, but the height limit was set to 60 m (approximately 20 storeys) at sites characterized by moderate seismic hazard, and 40 m (approximately 13 storeys) for high seismic hazard sites.

FAILURE MECHANISMS FOR RMSW SYSTEMS

Failure mechanisms for RM shear walls (RMSWs) can be classified as ductile failure (DF), diagonal shear failure (S), shear-flexure failure (SF), sliding failure (SL), toe-crushing or web-crushing failure (TC), bar-buckling (BB) and bar-fracture failure (BF), rocking (RO), and lateral instability (LI) [9]. The type of failure mechanism affects the seismic behavior of RMSWs in terms of the lateral strength, ductility, ultimate drift capacity, and strength degradation rate. In this paper, failure mechanisms corresponding to two distinct stages, namely the maximum strength and failure, defined as 80% of the maximum strength, are defined as primary failure mechanism (PF) and secondary failure mechanism (SF), respectively. The sequence of development of failure

mechanisms in RMSWs is complex, and it is common that more than two failure mechanisms occur before the collapse takes place (Figure 1). According to Robazza et al. [9], the primary failure mechanism governs the strength of a RMSW, while the secondary failure mechanism characterizes failure after the primary failure mechanism has been initiated, as illustrated in Figure 1.

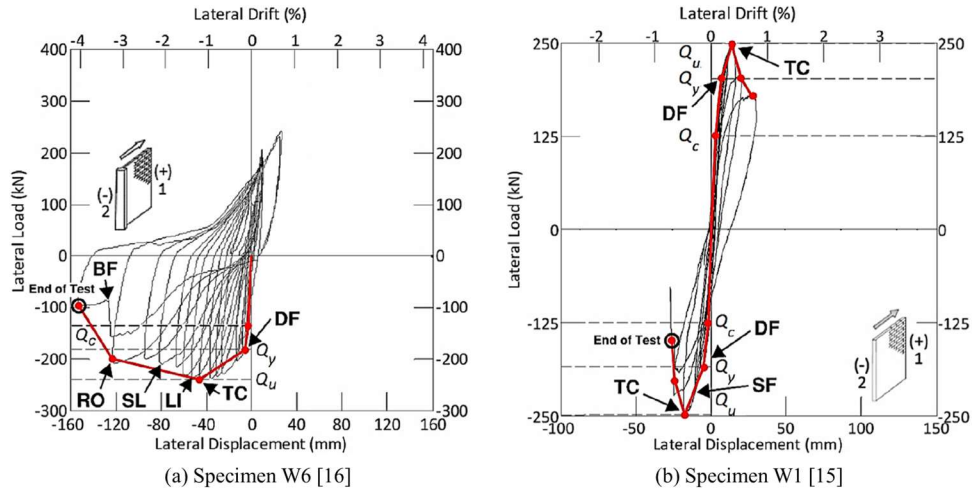


Figure 1: Hysteresis loops and failure sequence of RMSWs [9]

REVIEW OF COMPONENT-LEVEL TESTS ON SLENDER RMSWS

Summary of database

Important parameters influencing the behaviour of TRM shear walls have been identified by performing a review of past experimental research studies. In total, 60 wall specimens from 11 experimental studies [10-20] were selected based on the following criteria: i) shear span ratio (M/Vl_w) higher than 1.5, ii) ductile failure mode (DF) as the primary failure mechanism, and iii) reversed cyclic testing until the failure (drift ratio corresponding to 80% maximum lateral strength). Out of the selected specimens, 38 have a rectangular section and 22 have boundary elements (BE). Detailed information related to these specimens is summarized in Tables 1 and 2. Note that ρ_{BE} represents the ratio of flexural reinforcement area and the gross cross-sectional area of a BE ($\rho_{BE} = A_{s,BE}/A_{BE}$). The aspect ratios of all the specimens with rectangular section are equal to their shear span ratios.

Figure 2 shows histograms of design parameters of selected specimens. Limited field applications of TRM buildings in Canada can be partially attributed to scarcity of past experimental research studies on ductile RMSWs with dominant flexural behaviour, and aspect ratio higher than 2.0. Majority of Canadian experimental research studies were performed on ductile RMSWs with a rectangular cross-section [11-13, 15, 16]. Figure 2(c) shows that most research studies related to seismic behaviour of RMSWs were focused on testing fully grouted (FG) specimens. Research evidence on partially grouted (PG) RMSWs is very limited [11]. Only 3 slender RMSW specimens are reported in this paper. Figure 2(f) indicates that most research studies focus on the low axial stress level which is not representative of TRM buildings.

Table 1: Experimental database of RMSW specimens without boundary elements

| ID | Geometry | | | | Material (MPa) | | | Detailing (%) | | | Experimental Results | | |
|---------------------------------|-------------|-----------------|-------------------|-------------------|----------------|----------|----------|---------------|----------|----------------------|----------------------|-------------------|-------|
| | h (cm) | $\frac{h}{l_w}$ | $\frac{h_u}{t_w}$ | $\frac{l_w}{t_w}$ | f'_m | f_{yv} | f_{yh} | ρ_v | ρ_h | $\frac{P}{A_g f'_m}$ | V_{peak} (kN) | δ_u (%) | PF/SF |
| Priestley and Elder (1982) [10] | | | | | | | | | | | | | |
| Wall 1 | 540 | 2.3 | 14.3 | 10.5 | 26.9 | 434 | 322 | 0.72 | 0.40 | 7 | 323 | 0.90 | DF/TC |
| Wall 2 | 540 | 2.3 | 14.3 | 10.5 | 26.9 | 434 | 322 | 0.72 | 0.40 | 7 | 326 | 1.30 | DF/SL |
| Wall 3 | 540 | 2.3 | 14.3 | 10.5 | 26.9 | 434 | 322 | 0.72 | 0.40 | 3 | 268 | 1.60 | DF/TC |
| Shedid et al. (2005) [11] | | | | | | | | | | | | | |
| Wall 1 ^P | 360 | 2.0 | 19.0 | 9.5 | 15.2 | - | - | 1.31 | 0.26 | 0 | 274 | 0.60 | DF/TC |
| Wall 2 ^P | 360 | 2.0 | 19.0 | 9.5 | 15.2 | - | - | 1.31 | 0.26 | 0 | 360 | 1.30 | DF/TC |
| Wall 3 ^P | 360 | 2.0 | 19.0 | 9.5 | 15.2 | - | - | 0.73 | 0.13 | 0 | 242 | 1.80 | DF/TC |
| Shedid et al. (2008) [12] | | | | | | | | | | | | | |
| 1 | 360 | 2.0 | 9.5 | 9.5 | 14.8 | 502 | 491 | 0.29 | 0.08 | 0 | 143 | 2.15 | DF/TC |
| 2 | 360 | 2.0 | 9.5 | 9.5 | 14.8 | 502 | 491 | 0.78 | 0.13 | 0 | 265 | 1.80 | DF/TC |
| 3 | 360 | 2.0 | 9.5 | 9.5 | 14.8 | 502 | 491 | 0.73 | 0.13 | 0 | 242 | 1.30 | DF/TC |
| 4 | 360 | 2.0 | 9.5 | 9.5 | 14.8 | 502 | 491 | 1.31 | 0.26 | 0 | 360 | 1.51 | DF/TC |
| 5 | 360 | 2.0 | 9.5 | 9.5 | 14.8 | 502 | 491 | 1.31 | 0.26 | 5 | 377 | 1.31 | DF/TC |
| 6 | 360 | 2.0 | 9.5 | 9.5 | 14.8 | 624 | 491 | 1.31 | 0.26 | 10 | 541 | 1.73 | DF/TC |
| Shedid et al. (2010) [13] | | | | | | | | | | | | | |
| W1 | 399 | 2.2 | 13.7 | 20.0 | 16.4 | 495 | 534 | 1.17 | 0.30 | 7 | 177 | 1.11 | DF/TC |
| W4 | 266 | 1.5 | 13.7 | 20.0 | 16.4 | 495 | 534 | 1.17 | 0.60 | 6 | 265 | 1.07 | DF/TC |
| Ahmadi et al. (2014) [14] | | | | | | | | | | | | | |
| WSU-W-01A | 203 | 2.0 | 10.0 | 5.0 | 19 | 456 | 456 | 0.70 | 0.31 | 6 | 183 | 2.80 | - |
| WSU-W-01B | 203 | 2.0 | 10.0 | 5.0 | 21 | 446 | 446 | 0.70 | 0.31 | 6 | 201 | 2.10 | - |
| WSU-W-02A | 203 | 2.0 | 10.0 | 5.0 | 19 | 456 | 456 | 0.31 | 0.31 | 13 | 166 | 2.33 | - |
| WSU-W-02B | 203 | 2.0 | 10.0 | 5.0 | 21 | 450 | 450 | 0.31 | 0.31 | 13 | 124 | 1.50 | - |
| UT-W-13 | 366 | 3.0 | 6.0 | 6.0 | 31 | 421 | 421 | 0.70 | 0.16 | 5 | 142 | 1.84 | - |
| UT-W-14 | 366 | 3.0 | 6.0 | 6.0 | 23 | 448 | 448 | 0.31 | 0.16 | 10 | 108 | 2.91 | - |
| UT-W-15 | 366 | 3.0 | 6.0 | 6.0 | 23 | 421 | 421 | 0.70 | 0.16 | 10 | 160 | 2.11 | - |
| UT-W-16 | 366 | 3.0 | 6.0 | 6.0 | 23 | 448 | 448 | 0.31 | 0.16 | 15 | 121 | 2.10 | - |
| UT-W-17 | 366 | 4.5 | 4.0 | 4.0 | 29 | 421 | 421 | 0.70 | 0.31 | 5 | 64 | 4.51 | - |
| UT-W-18 | 366 | 4.5 | 4.0 | 4.0 | 29 | 448 | 448 | 0.31 | 0.31 | 10 | 42 | 3.14 | - |
| UT-W-19 | 366 | 4.5 | 4.0 | 4.0 | 23 | 421 | 421 | 0.70 | 0.16 | 10 | 78 | 3.42 | - |
| UT-W-20 | 366 | 4.5 | 4.0 | 4.0 | 23 | 448 | 448 | 0.31 | 0.16 | 15 | 63 | 2.83 | - |
| WSU-W-07 | 203 | 2.0 | 10.0 | 5.0 | 21 | 450 | 450 | 0.31 | 0.31 | 0 | 79 | 2.41 | - |
| WSU-W-08 | 203 | 2.0 | 10.0 | 5.0 | 21 | 455 | 455 | 0.31 | 0.31 | 6 | 139 | 2.43 | - |
| WSU-W-09 | 203 | 2.0 | 10.0 | 5.0 | 16 | 455 | 455 | 0.47 | 0.31 | 6 | 164 | 2.28 | - |
| WSU-W-31 | 284 | 2.0 | 14.0 | 7.0 | 16 | 465 | 465 | 0.70 | 0.16 | 0 | 196 | 2.51 | DF/SF |
| WSU-W-32 | 284 | 2.0 | 14.0 | 7.0 | 16 | 465 | 465 | 0.39 | 0.34 | 0 | 263 | 2.80 | DF/TC |
| WSU-W-33 | 284 | 2.0 | 14.0 | 7.0 | 16 | 465 | 465 | 0.39 | 0.34 | 6 | 313 | 2.70 | - |
| Robazza et al. (2018) [15] | | | | | | | | | | | | | |
| W1 | 380 | 15 | 27.1 | 18.6 | 23.4 | 484 | 484 | 0.33 | 0.36 | 8 | 251 | 0.56 | DF/SF |
| W2 | 380 | 1.5 | 27.1 | 18.6 | 23.4 | 512 | 512 | 0.33 | 0.36 | 0 | 217 | 1.82 | DF/LI |
| W3 | 400 | 1.5 | 21.1 | 13.7 | 27.1 | 508 | 508 | 0.24 | 0.26 | 0 | 206 | 2.08 | DF/RO |
| W4 | 400 | 2.9 | 21.1 | 7.4 | 27.1 | 465 | 465 | 0.15 | 0.26 | 0 | 43 | 1.84 | DF/BF |
| W5 | 400 | 1.5 | 28.6 | 18.6 | 27.1 | 506 | 506 | 0.33 | 0.36 | 0 | 189 | 0.54 | DF/TC |
| Robazza et al. (2019) [16] | | | | | | | | | | | | | |
| W8 | 400 | 1.5 | 21.1 | 13.7 | 26.4 | 499 | 499 | 0.24 | 0.26 | 0 | 225 | 1.88 | DF/TC |

Notes: h -wall height, l_w -wall length, h_u -unsupported wall height, t_w -wall thickness, f'_m - masonry compressive strength, f_{yv} -yield strength of vertical reinforcement, f_{yh} -yield strength of horizontal

reinforcement, ρ_v -area ratio of vertical reinforcement, ρ_h -area ratio of horizontal reinforcement, P -axial load, A_g -gross area of wall section, V_{peak} -maximum strength and δ_u -drift at $0.8 V_{peak}$ also denotes as the drift capacity, ^P = Partially grouted, - denotes that researchers did not report specific data.

Table 2: Experimental database of RMSW specimens with boundary elements.

| ID | Geometry | | | | Material (MPa) | | | | Detailing (%) | | | | Experimental Results | | |
|-------------------------------------|-------------|-----------------|-------------------|-------------------|----------------|----------|----------|-----------|---------------|----------|-------------|----------------------|----------------------|-------------------|-------|
| | h (cm) | $\frac{h}{l_w}$ | $\frac{h_u}{t_w}$ | $\frac{l_w}{t_w}$ | f'_m | f_{yv} | f_{yh} | f_{yBE} | ρ_v | ρ_h | ρ_{BE} | $\frac{P}{A_g f'_m}$ | V_{peak} (kN) | δ_u (%) | PF/SF |
| Shedid et al. (2010) [13] | | | | | | | | | | | | | | | |
| W2 ¹ | 399 | 2.2 | 13.7 | 6.4 | 16.4 | 495 | 534 | 495 | 0.55 | 0.3 | 1.18 | 5 | 151 | 1.56 | DF/BF |
| W3 | 399 | 2.2 | 13.7 | 9.7 | 16.4 | 495 | 534 | 495 | 0.55 | 0.3 | 1.17 | 5 | 152 | 2.34 | DF/TC |
| W5 ¹ | 266 | 1.5 | 13.7 | 6.4 | 16.4 | 495 | 534 | 495 | 0.55 | 0.6 | 1.18 | 5 | 245 | 1.47 | DF/BF |
| W6 | 266 | 1.5 | 13.7 | 9.7 | 16.4 | 495 | 534 | 495 | 0.55 | 0.6 | 1.17 | 5 | 241 | 1.81 | DF/TC |
| W7 ^a | 266 | 1.5 | 13.7 | 9.7 | 16.4 | 495 | 534 | 495 | 0.55 | 0.6 | 1.17 | 5 | 240 | 2.07 | DF/TC |
| Banting and El-Dakhkhni (2012) [17] | | | | | | | | | | | | | | | |
| W1 | 399 | 2.2 | 14.8 | 9.7 | 13.7 | 496 | 583 | 496 | 0.56 | 0.3 | 1.17 | 3 | 143 | 3.04 | DF/BF |
| W2 | 399 | 2.2 | 14.8 | 9.7 | 13.7 | 496 | 583 | 496 | 0.56 | 0.3 | 1.17 | 3 | 126 | 2.68 | DF/TC |
| W3 | 399 | 2.2 | 14.8 | 9.7 | 13.7 | 496 | 583 | 496 | 0.56 | 0.3 | 1.17 | 3 | 141 | 3.73 | DF/TC |
| W4 | 399 | 2.2 | 14.8 | 9.7 | 13.7 | 496 | 583 | 496 | 0.56 | 0.3 | 1.17 | 10 | 203 | 1.82 | DF/TC |
| Banting and El-Dakhkhni (2014) [18] | | | | | | | | | | | | | | | |
| Wall 1 | 399 | 1.5 | 44.3 | 14.4 | 14.9 | 496 | 583 | 496 | 0.51 | 0.3 | 1.17 | 6 | 314 | 1.75 | DF/TC |
| Wall 2 | 399 | 3.2 | 14.8 | 6.7 | 14.9 | 496 | 583 | 496 | 0.69 | 0.3 | 1.17 | 6 | 94 | 3.56 | DF/BF |
| Wall 3 | 266 | 2.2 | 14.8 | 6.7 | 14.9 | 496 | 583 | 496 | 0.69 | 0.6 | 1.17 | 6 | 132 | 1.82 | DF/TC |
| Wall 4 | 266 | 2.2 | 14.8 | 6.7 | 14.9 | 496 | 583 | 496 | 1.17 | 0.6 | 1.17 | 6 | 176 | 2.15 | DF/TC |
| Wall 5 | 190 | 1.5 | 21.1 | 6.7 | 14.9 | 496 | 583 | 496 | 0.69 | 0.6 | 1.17 | 6 | 177 | 2.20 | DF/TC |
| Aly and Galal (2020a, b) [19], [20] | | | | | | | | | | | | | | | |
| W7 | 238 | 1.4 | 17.8 | 9.0 | 8.7 | 460 | 535 | 460 | 0.18 | 0.20 | 0.79 | 15 | 62 | 2.36 | DF/TC |
| W8 | 238 | 1.4 | 17.8 | 9.0 | 8.7 | 460 | 535 | 460 | 0.18 | 0.20 | 1.57 | 15 | 83 | 2.69 | DF/TC |
| W9 | 238 | 1.4 | 17.8 | 9.1 | 8.7 | 460 | 535 | 460 | 0.18 | 0.20 | 1.03 | 14 | 87 | 3.05 | DF/TC |
| W10 | 238 | 1.4 | 17.8 | 9.0 | 14.2 | 460 | 535 | 460 | 0.18 | 0.20 | 0.79 | 16 | 113 | 2.02 | DF/TC |
| W11 | 238 | 1.4 | 17.8 | 9.3 | 14.2 | 460 | 535 | 460 | 0.18 | 0.20 | 0.83 | 16 | 57 | 1.82 | DF/TC |
| W12 | 238 | 1.4 | 17.8 | 9.0 | 14.2 | 460 | 535 | 460 | 0.18 | 0.20 | 0.79 | 16 | 62 | 1.75 | DF/TC |
| Robazza et al. (2019) [16] | | | | | | | | | | | | | | | |
| W6 ^{b,T} | 400 | 1.5 | 21.1 | 13.7 | 26.4 | 505 | 505 | 505 | 0.27 | 0.26 | 0.54 | 0 | 241 | 1.70 | DF/LI |
| W7 ^T | 400 | 1.5 | 21.1 | 13.7 | 26.4 | 507 | 507 | 507 | 0.27 | 0.26 | 0.54 | 0 | 355 | 2.15 | DF/SL |

Notes: f_{yBE} -yield strength of flexural reinforcement in boundary elements.^a - with spiral lateral reinforcement, ^b- asymmetrically loaded, ¹ – flanged cross-section, ^T – T-shaped cross-section. The remaining specimens have a barbell-shaped cross-section.

Field applications of RM shear walls in Canadian construction practice are mostly based on standard blocks with 20 cm nominal thickness, and less commonly 25 cm blocks, hence most experimental research studies on full-scale RM walls used blocks with 20 and 25 cm nominal thickness (note that actual block thickness is by 10 mm less than nominal). There is a lack of experimental evidence on seismic behaviour of RM shear walls constructed using blocks with 30 cm nominal thickness, the largest block size available in the market. This is believed to be a research gap since 30 cm blocks are most suitable for seismic design applications for high-rise structures, particularly in the context of boundary elements since there is a potential for using integrated boundary elements (within blocks).

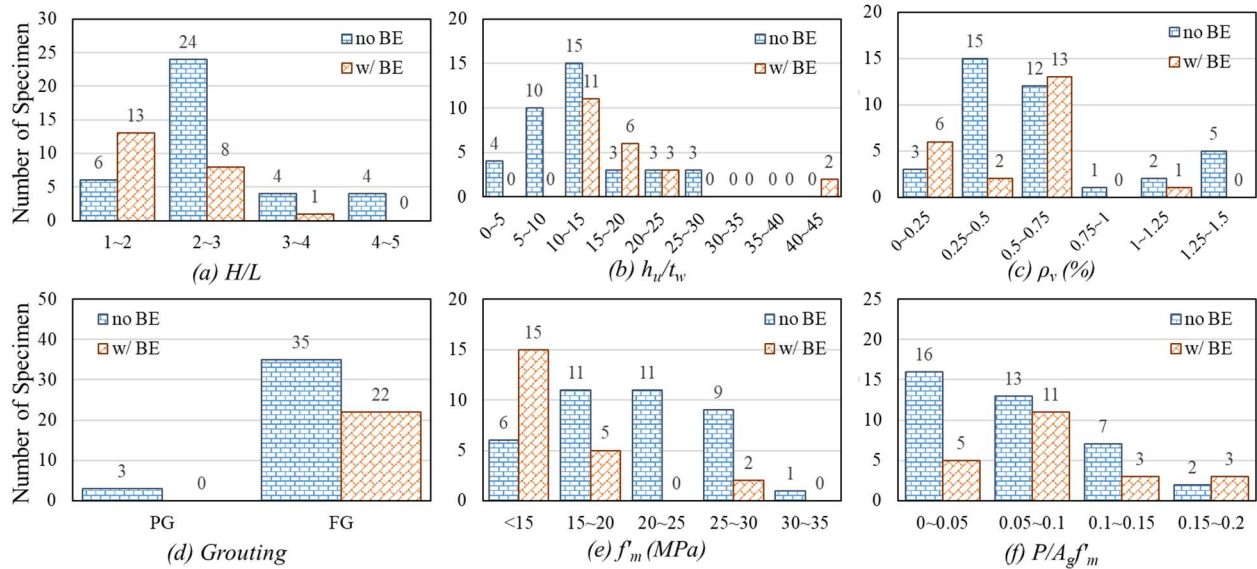


Figure 2: Histograms of selected test specimens presented in Tables 1 and 2

Key design parameters effecting the lateral drift capacity of TRM walls

Figure 3 shows the key parameters effecting the lateral drift capacity of TRM walls. The definition of lateral drift capacity δ_u is the drift corresponding to the 80% maximum strength of walls. Figure 3(a) shows that the aspect ratio (h/l_w) is positively correlated with the drift capacity. The behaviour of RMSWs with higher aspect ratios is not governed by the diagonal shear failure and shear-flexure failure, so the drift capacity is larger. On the other hand, Figure 3(b) and (d) show a negative correlation between length-to-thickness ratio (l_w/t_w), unsupported height-to-thickness ratio (h_u/t_w), and drift capacity. Robazza et al. [15] indicated that RMSWs with higher l_w/t_w and h_u/t_w ratios may experience lateral instability (LI) failure at relatively small drift levels.

Figure 3(c) presents a slightly positive correlation between the vertical reinforcement ratio ρ_v and drift capacity. Higher ρ_v prevents RMSWs from sliding failure and provides higher flexural strength for RMSWs. Figure 3(e) shows unclear trends for a correlation between axial stress level ($P/A_g f'_m$) and drift capacity, however Figure 3(f) shows a negative correlation between axial stress level and drift capacity for specimens from several testing program [10, 13, 14, 15, 17]. Figure 3(f) indicates that the drift capacity of RMSWs becomes smaller at higher axial stress levels. The

gravity load is expected to be higher for TRM buildings while the experimental data with axial stress level higher than $0.1f'_m$ is limited. Future research studies need to address the impact of high axial stress level on the seismic behaviour of TRM buildings.

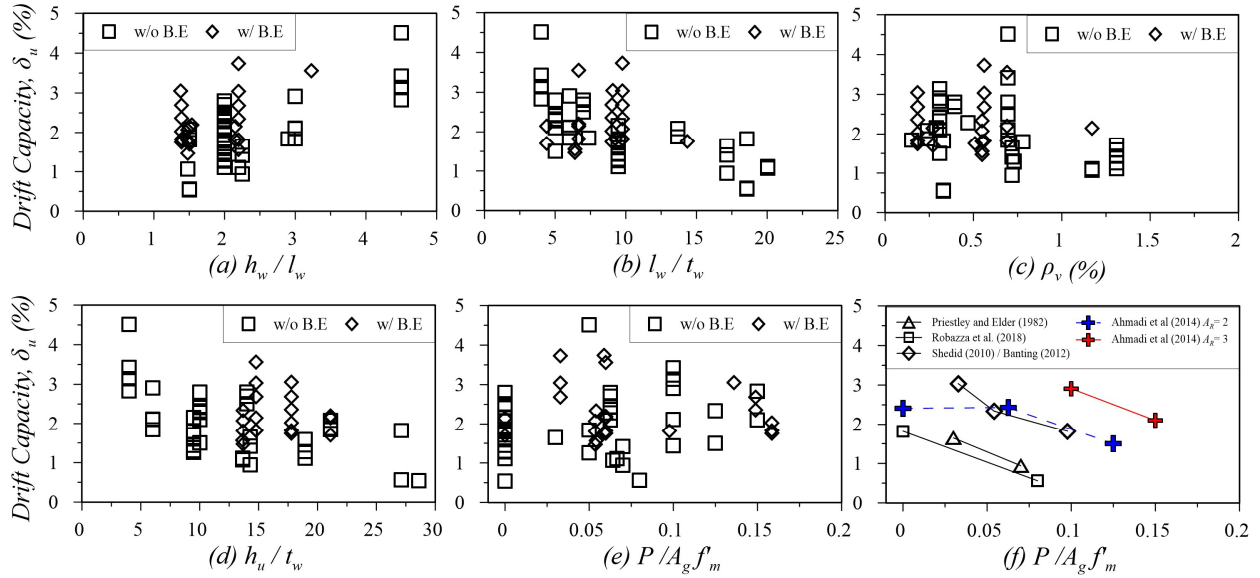


Figure 3: Effect of design parameters on the drift capacity

Other important parameters and impact of boundary elements

Figure 4(a) indicates that the level of wall shear stress is another important parameter affecting the drift capacity of RMSWs. The higher the shear stress, the lower the drift capacity. Furthermore, it can be observed that among the specimens subjected to similar shear stress level, drift capacities are higher for specimens with BEs. For the RMSWs with boundary elements, Figures 4(b) and 4(c) show that the flexural reinforcement ratio in the boundary elements ρ_{BE} and the area ratio of boundary elements A_{BE}/A_g are slightly positively correlated with the drift capacity. However, different shapes, detailing, confinement level, and layout of BEs affect the drift capacity [17][18], hence the impact of these two parameters cannot be easily quantified, as shown in Figures 3(e) and 3(f).

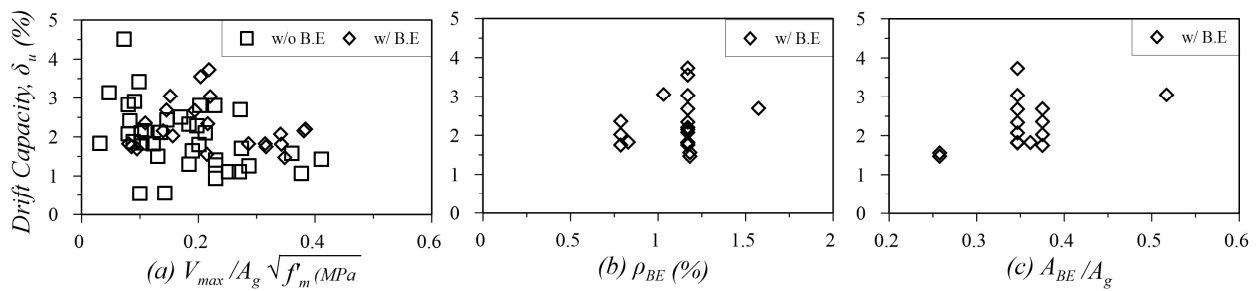


Figure 4: Effect of boundary elements on the drift capacity

SYSTEM-LEVEL TESTING OF RM BUILDINGS

System-level testing of RM buildings involves testing of building models subjected to quasi-static (reversed cyclic) loading, simulated earthquake excitation via shaking table, and hybrid numerical-experimental testing. There is a limited evidence related to system-level testing of RM buildings. Three 1/3rd scale specimens of a 2-storey prototype RM building were subjected to reversed quasi-static loading to observe the overall system behaviour [21][22][23]. The effect of asymmetric building layout and the interaction between slabs, coupled walls and flanged walls, the influence of wall-to-floor interaction and diaphragm rigidity, and the systematic behaviour of RMSWs with boundary elements were studied, respectively. For the dynamic systematic behaviour of RM buildings, 2- and 3-storey full-scale fully grouted RM building specimens were tested on a shaking table [24][25]. The results indicated that a shear failure unexpectedly occurred due to the wall-to-floor interaction. It was observed that rigid slabs shortened the shear span ratio of RM shear walls, caused unexpected shear failure, and reduced the ductility of RM wall system. Dynamic behaviour of a full-scale, one-storey, partially grouted RM building model was tested on a shake table [26]. Base sliding mechanism of the PGRM building specimen was observed prior to flexural and shear failure under an MCE level ground motion during the shake table test. The tallest full-scale RM building model was 8m high, but RM shear walls were designed as non-loadbearing walls [25]; similarly, three 1/3rd scale specimens [21][22][23] were not subjected to additional axial precompression. In addition to the axial stress level, scaling is another important issue for TRM building models with boundary elements due to challenges associated with placing of vertical reinforcement in scaled blocks within the boundary zones. Shaking table tests and quasi-static tests of RM building models provided useful results which contributed to understanding the seismic behaviour of RM buildings, however current experimental facilities limit abilities to test full-scale models of TRM buildings characterized by higher wall aspect ratios and higher axial stress levels.

Hybrid simulation testing approach offers a possible solution to this problem. Since the ductile slender RMSWs in TRM buildings are expected to experience flexural failure, the most significant damage is expected in the plastic hinge region at the wall base. It is possible to evaluate the systematic behaviour of TRM buildings by testing only the lower portion of slender RMSWs and simulate the remaining portion of the wall and entire building through numerical simulations, as shown in Figure 5. In this manner, hybrid testing reduces the cost of specimens and the demand for expensive experimental facilities. Recently, Miraglia et al. [27] developed a framework of hybrid simulation testing for a two-storey prototype unreinforced masonry (URM) structure. The first storey of the URM structure was physically tested in the laboratory, while the second storey was numerically modeled by linear four-node 2D solid elements in MATLAB. The loading system was able to control three degrees of freedom (DOF) for the test specimens (2 translational DOFs and 1 rotational DOF). The study was focused on in-plane behavior of URM test specimens subjected to 10% axial stress level.

The research project which is currently at the initial stage at the University of British Columbia (UBC) intends to examine seismic response of TRM shear walls through a robust experimental and analytical research program. The specimens are characterized by high aspect ratios,

corresponding to mid-rise to tall buildings and are designed to behave in flexure-dominant manner. Seismic response of TRM shear walls will be examined at the material, component, and system levels. Material testing will be performed to establish the mechanical properties and characterizing relevant stress-strain relationships of hollow concrete block units, mortar, and masonry prisms [28]. Subsequently, several specimens will be subjected to reversed cyclic loading to characterize seismic response of TRM walls at the component (sub-assembly) level. Detailed numerical simulations will be performed to simulate the response of test specimens [29]. A hybrid experimental and numerical simulation will be performed at the system level to obtain the seismic response of a TRM building subjected to earthquake excitation [30]. Wall-to-floor interaction due to seismic loading will be taken into account in designing the specimens. This is believed to be the first application of hybrid simulation technology for studying the seismic response of TRM buildings.

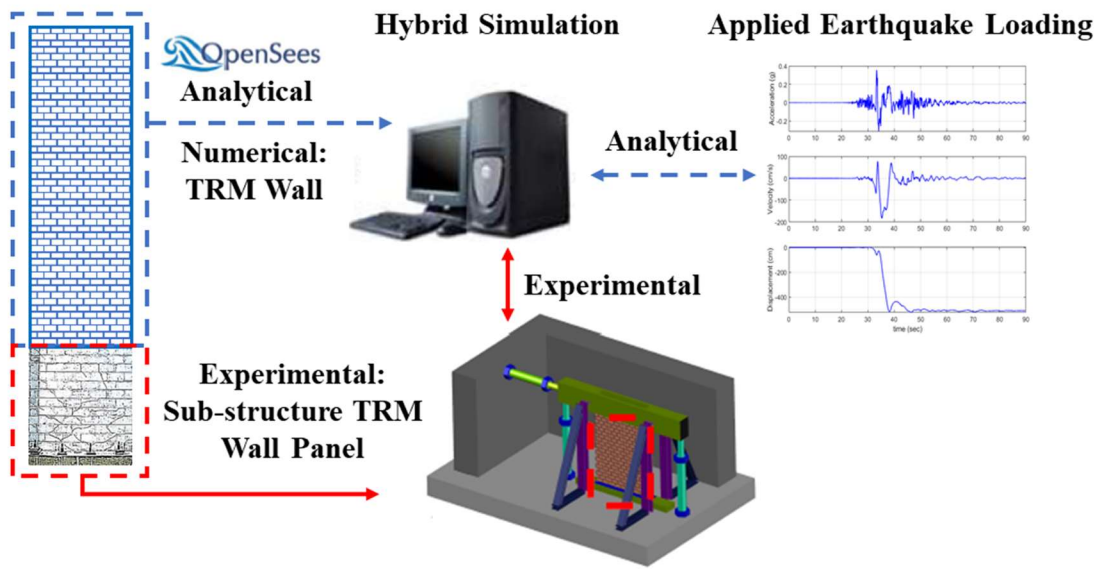


Figure 5: Hybrid simulation approach for TRM buildings

CONCLUSION

A review of experimental research studies on RM wall components and systems is presented in the paper. The results of previous experimental studies on individual RM walls (component testing) indicated that the axial stress level and aspect ratio are important parameters affecting the behaviour and drift capacity of RMSWs, while the system-level testing of RM building models pointed out that the wall-to-floor interaction influences behaviour of RMSW structures. Hybrid simulation testing is a promising approach for understanding the seismic response of TRM buildings because it is not constrained by the capacity of experimental facilities. Prior to the hybrid testing, it is required to study the behaviour of individual walls in order to develop a reliable numerical model of RM building. An ongoing research project at UBC will utilize hybrid testing approach to examine seismic behaviour of TRM buildings for applications in Canada and other countries.

ACKNOWLEDGEMENTS

The authors would like to acknowledge the support from NSERC Alliance Grant, and from industry partners Canada Masonry Design Centre (CMDC) and Canadian Concrete Masonry Producers Association (CCMPA).

REFERENCES

- [1] Drysdale, R.G., and Hamid, A.A. (2005). *Masonry Structures: Behaviour and Design*, Canadian Edition, Canada Masonry Design Centre, Mississauga, ON, Canada.
- [2] Hamid, A. (2018). *Masonry Structures: Behaviour and Design*. Fourth Edition, The Masonry Society, USA.
- [3] Corrêa, M.R.S. (2012). Masonry Engineering in Brazil: Past Development, Current Overview, Future Improvements. *Proc., 15th Int. Brick and Block Masonry Conf.*, Florianópolis, Brazil.
- [4] Wang, F. L., Zhang, X. C., and Zhu, F. (2016). Research progress and low-carbon property of reinforced concrete block masonry structures in China. *Proc., 16th Int. Brick and Block Masonry Conf.*, Padova, Italy.
- [5] El-Dakhkhni, W., and Ashour, A. (2017). Seismic response of reinforced concrete masonry shear-wall components and systems: State of the art. *J. Struct. Eng.* 143 (9): 03117001. [https://doi.org/10.1061/\(ASCE\)ST.1943-541X.0001840](https://doi.org/10.1061/(ASCE)ST.1943-541X.0001840).
- [6] CSA S304-14 (2014). Design of Masonry Structures, *Canadian Standards Association*, Mississauga, ON, Canada.
- [7] NRC (2015). National Building Code of Canada 2015, *National Research Council*, Ottawa, ON, Canada.
- [8] Brzev, S. and Anderson, D.L. (2018). *Seismic Design Guide for Masonry Buildings*. Second Edition, Canadian Concrete Masonry Producers Association, Toronto, Ontario, Canada (www.ccmppa.ca).
- [9] Robazza, B. R. et al. (2020). Seismic behaviour and design code provisions for predicting the capacity of ductile slender reinforced masonry shear walls. *Engineering Structures*, 222, 110992.
- [10] Priestley, M. N., D. McG. Elder. (1982). *Seismic Behaviour of Slender Concrete Masonry Shear Walls*. Christchurch, New Zealand: Dept. of Civil Engineering, Univ. of Canterbury.
- [11] Shedid, M., A.A. Hamid and R. G. Drysdale. (2005). Ductility of Reinforced Masonry Shear Walls and Impact of Incomplete Grouting. *Proc., 10th Canadian Masonry Symposium*. Banff, Alberta.
- [12] Shedid, M. T., Drysdale, R. G., and El-Dakhkhni, W. W. (2008). Behavior of Fully Grouted Reinforced Concrete Masonry Shear Walls Failing in Flexure: Experimental Results. *Journal of Structural Engineering*, 134(11), 1754–1767.
- [13] Shedid, M. T., El-Dakhkhni, W. W., and Drysdale, R. G. (2010). Alternative Strategies to Enhance the Seismic Performance of Reinforced Concrete-Block Shear Wall Systems. *Journal of Structural Engineering*, 136(6), 676-689.
- [14] Ahmadi, F. et al. (2014). Seismic Performance of Cantilever-Reinforced Concrete Masonry Shear Walls. *Journal of Structural Engineering*, 140(9), 04014051.
- [15] Robazza, B. R. et al. (2018). Out-of-Plane Behavior of Slender Reinforced Masonry Shear Walls under In-Plane Loading: Experimental Investigation. *Journal of Structural Engineering*, 144(3), 04018008.

- [16] Robazza, B. R., Yang, T. Y., Brzev, S., Elwood, K. J., Anderson, D. L., and McEwen, W. (2019). Response of slender reinforced masonry shear walls with flanged boundary elements under in-plane lateral loading: An experimental study. *Engineering Structures*, 190, 389–409.
- [17] Banting, B. R., and El-Dakhakhni, W. W. (2012). Force- and Displacement-Based Seismic Performance Parameters for Reinforced Masonry Structural Walls with Boundary Elements. *Journal of Structural Engineering*, 138(12), 1477–1491.
- [18] Banting, B. R., and El-Dakhakhni, W. W. (2014). Seismic Performance Quantification of Reinforced Masonry Structural Walls with Boundary Elements. *Journal of Structural Engineering*, 140(5), 04014001.
- [19] Aly, N., and Galal, K. (2020a). In-plane cyclic response of high-rise reinforced concrete masonry structural walls with boundary elements. *Engineering Structures*, 219, 110771.
- [20] Aly, N., and Galal, K. (2020b). Experimental Investigation of Axial Load and Detailing Effects on the Inelastic Response of Reinforced-Concrete Masonry Structural Walls with Boundary Elements. *Journal of Structural Engineering*, 146(12), 04020259.
- [21] Heerema, P. et al. (2015). *System-Level Seismic Performance Assessment of an Asymmetrical Reinforced Concrete Block Shear Wall Building*. *Journal of Structural Engineering*, 141(12), 04015047.
- [22] Ashour, A., El-Dakhakhni, W., and Shedid, M. (2016). Experimental Evaluation of the System-Level Seismic Performance and Robustness of an Asymmetrical Reinforced Concrete Block Building. *Journal of Structural Engineering*, 142(10), 04016072.
- [23] Ezzeldin, M. (2017). *System-level seismic performance quantification of reinforced masonry buildings with boundary elements*. Ph.D. thesis, McMaster Univ., Hamilton, ON, Canada.
- [24] Mavros, M., Ahmadi, F., Shing, P. B., Klingner, R. E., McLean, D., and Stavridis, A. (2016). Shake-Table Tests of a Full-Scale Two-Story Shear-Dominated Reinforced Masonry Wall Structure. *Journal of Structural Engineering*, 142(10), 04016078.
- [25] Stavridis, A., Ahmadi, F., Mavros, M., Shing, P. B., Klingner, R. E., and McLean, D. (2016). Shake-Table Tests of a Full-Scale Three-Story Reinforced Masonry Shear Wall Structure. *Journal of Structural Engineering*, 142(10), 04016074.
- [26] Koutras, A. A., and Shing, P. B. (2020). Seismic behavior of a partially grouted reinforced masonry structure: Shake-table testing and numerical analyses. *Earthquake Engineering & Structural Dynamics*, 49(11), 1115–1136.
- [27] Miraglia, G., Petrovic, M., Abbiati, G., Mojsilovic, N., and Stojadinovic, B. (2020). A model-order reduction framework for hybrid simulation based on component-mode synthesis. *Earthquake Engineering & Structural Dynamics*, 49(8), 737–753.
- [28] Mohamad, G., Lourenco, P.B. and Roman, H.R. (2006). Mechanics of Hollow Concrete Block Masonry Prisms under Compression: Review and Prospects, *Cement & Concrete Composites*, 29: 181–192.
- [29] Abdel-Latif, A. et al. (2015). Modelling of Reinforced Masonry Structural Walls Under Lateral Loads. *Proceedings of the 12th North American Masonry Conference*, Denver, CO, USA.
- [30] Ahmadi, F. et al. (2015). Displacement-based seismic design for reinforced masonry shear-wall structures. Part 1: Background and trial application. *Earthquake Spectra*, 31(2): 969–998.